

Linear and Nonlinear Optical Properties of Diiron μ -Vinylcarbyne Acceptor and Stilbenyl Donor Based Chromophores

Tony Farrell,[†] Timo Meyer-Friedrichsen,[‡] Jürgen Heck,^{*,‡} and Anthony R. Manning^{*,†}

University College Dublin, Belfield, Dublin 4, Ireland, and Institut für Anorganische und Angewandte Chemie, Universität Hamburg, Martin-Luther-King-Platz 6, D-20146 Hamburg, Germany

Received February 8, 2000

Ionic $[(\text{CpFeCO})_2(\mu\text{-CO})(\mu\text{-CCH=CH-})]^+$ fragments were used as electron acceptors in combination with *para*-substituted stilbenyl donors to form push–pull chromophores. These μ -vinylcarbyne salts were prepared by two complementary procedures: (a) the direct condensation of the μ -ethyldiyne complex $[(\text{CpFeCO})_2(\mu\text{-CO})(\mu\text{-CCH}_3)]\text{[BF}_4\text{]}$ with various stilbenyl aldehydes and (b) the preparation and reaction of the neutral aldehyde $[(\text{CpFeCO})_2(\mu\text{-CO})(\mu\text{-C=CHCH}_2\text{C}_6\text{H}_4\text{CHO})]$ with Wittig reagents followed by hydride abstraction using $[\text{Ph}_3\text{C}]\text{[BF}_4\text{]}$. While the series did exhibit high nonlinear activity (measured by hyper-Rayleigh scattering techniques), fluorescence checks revealed emission bands in the proximity of the second harmonic signal due to two-photon absorption.

1. Introduction

The design of second-order nonlinear optical (NLO) materials is now quite advanced, and certain criteria have been established as being essential for the exhibition of large first hyperpolarizabilities.¹ While most efforts have concentrated on organic chromophores, there is growing interest in organometallic systems.² It has been suggested that coplanarity of the metals with the π -electrons may benefit NLO efficiency.³ Recent studies concur with this proposal,⁴ and the largest hyperpolarizability reported to date for an organometallic compound is that of a Zn^{II} porphyrin donor–acceptor system.⁵

In this report we describe the synthesis of a series of donor–acceptor chromophores utilizing the cationic diiron moiety $[(\text{CpFeCO})_2(\mu\text{-CO})(\mu\text{-CCH=CHR})]^+$ as the electron acceptor. Theoretical⁶ and experimental⁷ re-

search has indicated that conjugation between the Fe₂–(μ -C) unit and the substituted vinyl system is maintained throughout rotation, and it was hoped that this phenomenon may also be beneficial to optical nonlinearity.

2. Results and Discussion

2.1. Synthesis. The stilbenyl aldehydes **1–4** were prepared by Wittig condensation of terephthalaldehyde diethylacetal with equimolar amounts of phosphorus ylides, prepared from the reaction of the phosphonium salts⁸ and *t*-BuOK, forming the acetals $\text{RCH=CHC}_6\text{H}_4\text{-CH(OEt)}_2$. Treatment of the crude reaction mixture with aqueous HCl afforded after workup the aldehydes in Scheme 1. The phosphonate **7** was prepared in quantitative yield by reacting 2-bromo-5-(chloromethyl)thiophene⁹ with 1.05 equiv of triethyl phosphite at 140 °C for 6 h. Reaction of **7** with the aldehydes (dimethylamino)benzaldehyde and (dimethylamino)cinnamaldehyde followed by bromine/lithium exchange and DMF quenching yielded after the usual workup the all-trans isomers 4-Me₂NC₆H₄CH=CH(th)CHO (**5**) and 4-Me₂NC₆H₄CH=CHCH=CH(th)CHO (**6**) (where th denotes 2,5-disubstituted thiophene). All of the compounds exhibit ¹H NMR signals associated with the aryl protons, and the ethylene bridge signals appear as doublets with coupling constants of $J > 16$ Hz, in accord with a trans stereochemistry.

These aldehydes were condensed with the μ -ethyldiyne complex $[(\text{CpFeCO})_2(\mu\text{-CO})(\mu\text{-CCH}_3)]\text{[BF}_4\text{]}^{10}$ (**8**) in CH₂Cl₂ at 35 °C for 12 h to yield the intensely colored

[†] University College Dublin.

[‡] Universität Hamburg.

(1) Marder, S. R.; Perry, J. W. *Adv. Mater.* **1993**, *5*, 804.

(2) (a) In *Nonlinear Optics Of Organic Molecules and Polymers*; Nalwa, H. S., Miyata, S., Eds.; CRC Press: New York, 1997. (b) Boyd, R. W. In *Nonlinear Optics*; Academic Press: New York, 1992. (c) Prasad, P. N.; Williams, D. J. In *Nonlinear Optical Effects in Molecules & Polymers*; Wiley: New York, 1991. (d) Heck, J.; Dabek, S.; Meyer-Friedrichsen, T.; Wong, H. *Coord. Chem. Rev.* **1999**, *190–192*, 1217. (e) Verbiest, T.; Houbrechts, S.; Kauranen, M.; Clays, K.; Persoons, A. *J. Mater. Chem.* **1997**, *7*(11), 2175. (f) Whittall, I. R.; McDonagh, A. M.; Humphrey, M. G. *Adv. Organomet. Chem.* **1998**, *42*, 291.

(3) Calabrese, J. C.; Cheng, L.-T.; Green, M. L. H.; Marder, S. R. *J. Am. Chem. Soc.* **1991**, *113*, 7227.

(4) (a) Houbrechts, S.; Clays, K.; Persoons, A.; Cadierno, V.; Gamasa, M. P.; Gimeno, J. *Organometallics* **1996**, *15*, 5266. (b) Whittall, I. R.; Humphrey, M. G.; Persoons, A.; Houbrechts, S. *Organometallics* **1996**, *15*, 1935. (c) Dhenaut, C.; Ledoux, I.; Samuel, I. D.; Zyss, J.; Bourgault, M.; Bozec, H. L. *Nature* **1995**, *374*, 339.

(5) (a) Lecours, S. M.; Guan, H.-W.; Dimagno, S. G.; Wang, C. H.; Therien, M. J. *J. Am. Chem. Soc.* **1996**, *118*, 1497. (b) Priyadarshy, S.; Therien, M. J.; Beratan, D. N. *J. Am. Chem. Soc.* **1996**, *118*, 1504.

(6) Hall, M. B.; Fenske, R. F. *Inorg. Chem.* **1972**, *11*, 768.

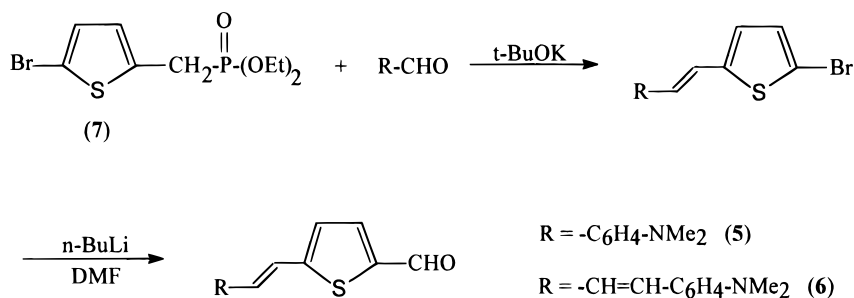
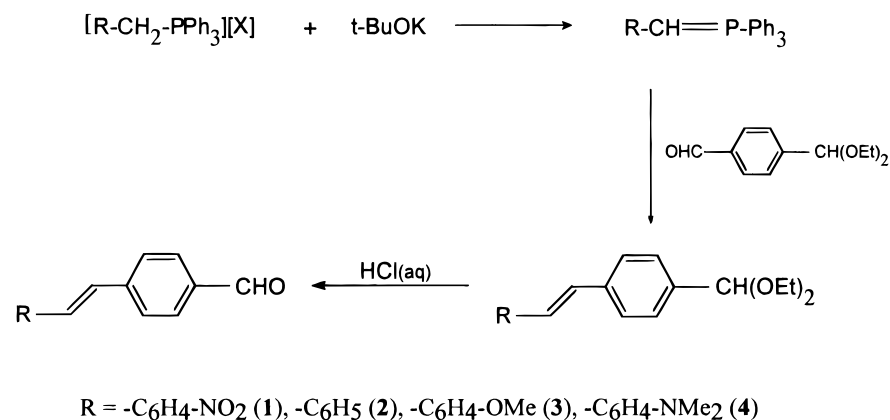
(7) Casey, C. P.; Konings, M. S. M. S.; Marder, S. R.; Takezawa, Y. *J. Organomet. Chem.* **1988**, *358*, 347.

(8) (a) Broos, R.; Anteunis, M. *Synth. Commun.* **1976**, *6*, 53. (b) Bredereck, H.; Simchen, G.; Griebenom, W. *Chem. Ber.* **1973**, *106*, 3732. (c) Kröhnke, F. *Chem. Ber.* **1950**, *83*, 291. (d) McDonald, R. N.; Campbell, T. W. *J. Org. Chem.* **1959**, *24*, 1969.

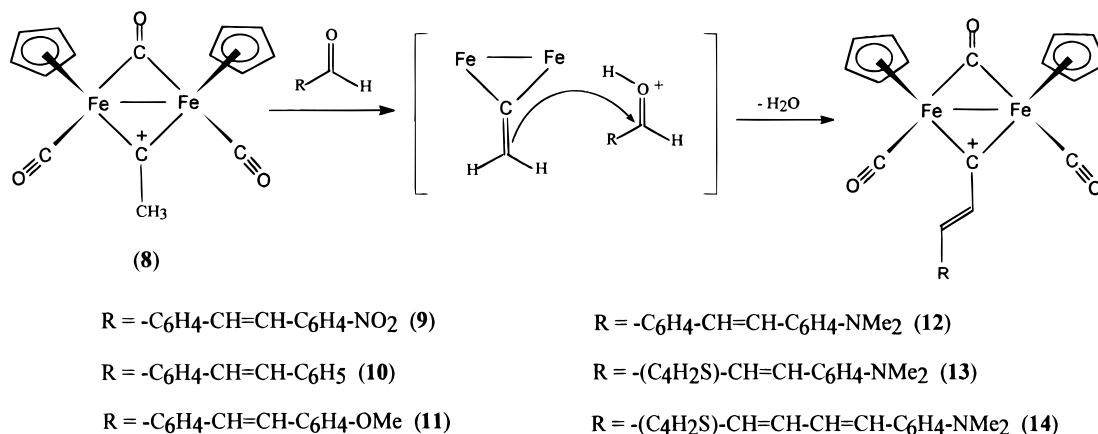
(9) Blicke, L. *J. Am. Chem. Soc.* **1946**, *68*, 1934.

(10) Nitay, M.; Priester, W.; Rosenblum, M. *J. Am. Chem. Soc.* **1978**, *100*, 3620.

Scheme 1. Synthesis of Aryl Aldehydes 1–6



Scheme 2. Reaction of 8 with Aldehydes



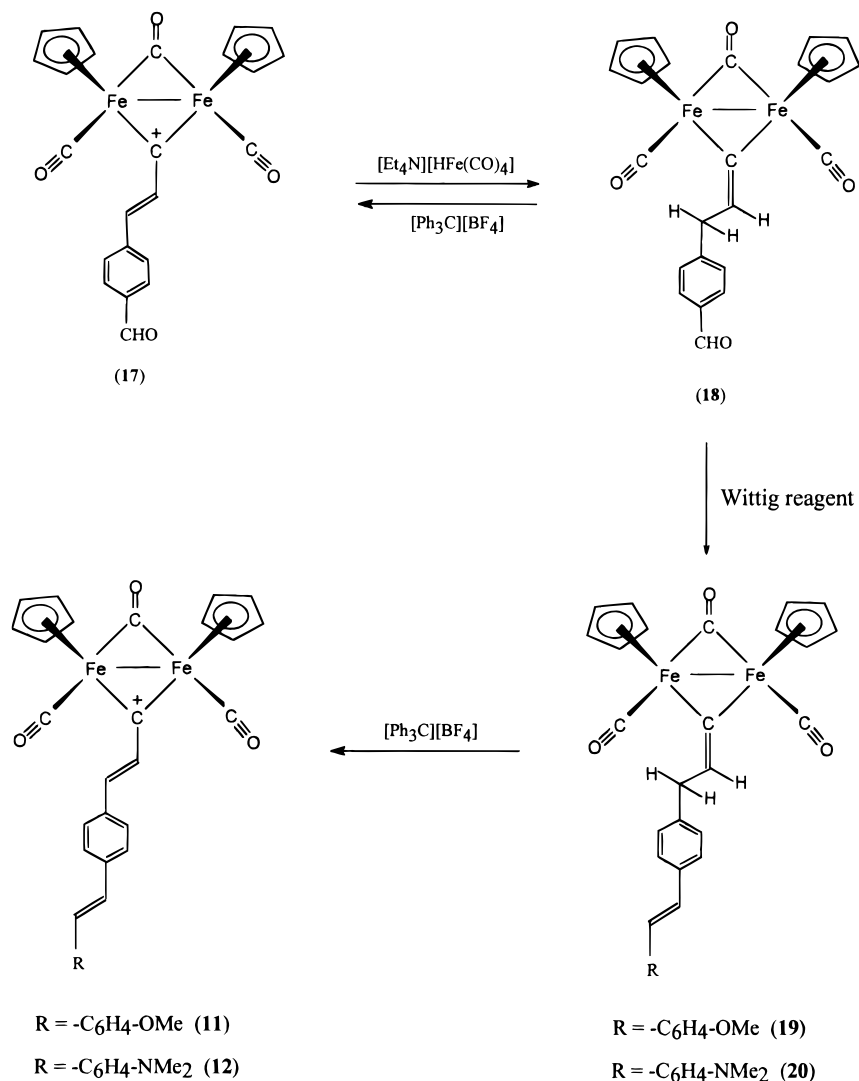
cationic vinyl carbyne complexes **9–14**. This reaction has been proposed to proceed via nucleophilic attack of a μ -alkenylidene complex (in equilibrium with **8**) on a protonated aldehyde followed by dehydration to generate the vinylcarbyne complex (Scheme 2).¹¹ Unfortunately when longer reaction times were necessary, product purification was often difficult due to the formation of [CpFe(CO)₃][BF₄]. Therefore, an alternative synthetic route was attempted whereby the diiron μ -alkenylidene aldehyde [(CpFeCO)₂(μ -CO)(μ -C=CHCH₂C₆H₄CHO)] (**18**) was prepared. Hence, a wide range of vinyl carbyne complexes are achievable from the reaction of **18** with Wittig reagents and subsequent allylic hydride abstraction with [Ph₃C][BF₄] (Scheme 3).

To achieve this, **8** was reacted with an excess of terephthalaldehyde in CH₂Cl₂ for 8 h. The precipitate

was filtered off, and concentration of the filtrate in THF yielded a microcrystalline solid which was identified from spectroscopy as the complex [(CpFeCO)₂(μ -CO)(μ -CCH=CHC₆H₄CHO)][BF₄] (**17**). The precipitate was characterized from ¹H NMR spectroscopy as the dication [(CpFeCO)₂(μ -CO)(μ -CCH=CHC₆H₄CH=CHC- μ)(μ -CO)-(CpFeCO)₂][BF₄]₂ (**16**), generated from the condensation of 2 equiv of **8** with terephthalaldehyde.

Casey et al. found that nucleophiles add regioselectively to vinyl carbyne complexes at the remote vinyl carbon to generate μ -alkenylidene complexes.¹¹ A variety of nucleophiles were reacted with **17** with the same regioselectivity to form neutral diiron complexes, but it

(11) Casey, C. P.; Konings, M. S.; Marder, S. R. *J. Organomet. Chem.* **1988**, 345, 125.

Scheme 3. Hydride Abstraction Route to Vinylcarbynes 11 and 12

was necessary to retain the aldehydic functional group for further reaction. The reaction of **17** with $[\text{Et}_4\text{N}][\text{HFe}(\text{CO})_4]$ ¹² produced the desired neutral diiron complex $[(\text{CpFeCO})_2(\mu\text{-CO})(\mu\text{-C}=\text{CHCH}_2\text{C}_6\text{H}_4\text{CHO})]$ (**18**) (Scheme 3). The addition of this hydride source to cationic diiron complexes gave ether-soluble neutral diiron complexes, while the byproduct was the ether-insoluble anionic $[\text{HFe}_3(\text{CO})_{11}]^-$, which was easily separated by filtration.¹³ Reaction of **18** with $[\text{Ph}_3\text{C}][\text{BF}_4]$ led to the reformation of **17**.

18 was reacted with the phosphonium salts $[4\text{-Me-OC}_6\text{H}_4\text{CH}_2\text{PPh}_3][\text{Cl}]$ ^{8a} and $[4\text{-Me}_2\text{NC}_6\text{H}_4\text{CH}_2\text{PPh}_3][\text{I}]$ ^{8b} in the presence of *t*-BuOK to yield the carbene complexes $[(\text{CpFeCO})_2(\mu\text{-CO})(\mu\text{-C}=\text{CHCH}_2\text{C}_6\text{H}_4\text{CH}=\text{CHC}_6\text{H}_4\text{-4-OMe})]$ (**19**) and $[(\text{CpFeCO})_2(\mu\text{-CO})(\mu\text{-C}=\text{CHCH}_2\text{C}_6\text{H}_4\text{-CH}=\text{CHC}_6\text{H}_4\text{-4-NMe}_2)]$ (**20**). The trans conformation of the bridging stilbenyl ligands of these diiron carbene complexes was confirmed by examination of the ¹H NMR coupling constants. Reaction of **19** and **20** with $[\text{Ph}_3\text{C}][\text{BF}_4]$ resulted in an immediate color change due to hydride abstraction from the allylic carbon and the formation of **11** and **12** (Scheme 3).

2.2. Crystal Structure of 17. Although suitable crystals of **9–14** could not be obtained, those of the

important intermediate $[(\text{CpFeCO})_2(\mu\text{-CO})(\mu\text{-CCH}=\text{CHC}_6\text{H}_4\text{-4-CHO})][\text{BF}_4]$ (**17**) were grown from a THF solution and subjected to an X-ray diffraction study. Results of the X-ray structure analysis are summarized in Table 1, and selected bond lengths and bond angles are presented in Table 2. The overall geometry is typical of such diiron cyclopentadienyl complexes with a cis disposition of the CpFeCO units bridged by a carbonyl and a vinylcarbyne ligand (Figure 1).^{7,14,15} The C14–C15 bond length of 142.8(7) pm and the C15–C16 bond length of 135.1(7) pm, which is typical of a double bond, reveals that the positive charge is essentially localized on the $\text{Fe}_2(\mu\text{-C})$ core in the solid state. In contrast to the crystal structure of $[(\text{CpFeCO})_2(\mu\text{-CO})(\mu\text{-CCH}=\text{CHC}_6\text{H}_4\text{CH}_3)][\text{BF}_4]$ ^{14a} there is a larger deviation from planarity (21.6°), between the vinyl group and the $\text{Fe}_2(\mu\text{-C})$ center. This may be a result of crystal packing rather than an electronic effect, as rotation of the ligand is not expected to diminish electronic interaction with the $\text{Fe}_2(\mu\text{-C})$ core. On the other hand, the 18.1° distortion

(13) Kao, S. C.; Lao, P. P. Y.; Pettit, R. *Organometallics* **1982**, *1*, 911.

(14) (a) Casey, C. P.; Konings, M. S.; Palermo, R. E.; Colborn, R. E. *J. Am. Chem. Soc.* **1985**, *107*, 5296. (b) Casey, C. P.; Konings, M. S.; Marder, S. R. *Polyhedron* **1988**, *7*, 881.

(15) Etienne, M.; Talarmin, J.; Toupet, L. *Organometallics* **1992**, *11*, 2058.

(12) Cole, T. E.; Pettit, R. *Tetrahedron Lett.* **1979**, 781.

Table 1. Crystal Data and Structure Refinement Details for 17

empirical formula	C ₂₄ H ₁₉ BCl ₂ Fe ₂ O ₄
fw	640.80
temp (K)	293
λ (pm)	7.1073
cryst syst	triclinic
space group	<i>P</i> 1
unit cell dimens	
<i>a</i> (Å)	9.722(2)
<i>b</i> (Å)	11.306(2)
<i>c</i> (Å)	12.858(3)
α (deg)	108.10(3)
β (deg)	94.59(3)
γ (deg)	100.84(3)
<i>V</i> (Å ³)	1304.7(5)
<i>Z</i>	2
ρ_{exptl} (g/cm ³)	1.631
abs coeff (mm ⁻¹)	1.374
<i>F</i> (000)	644
cryst size (mm ³)	0.3 × 0.2 × 0.2
$\theta_{\text{min,max}}$ (deg)	2.53–27.57
index ranges	–1 ≤ <i>h</i> ≤ 12 –14 ≤ <i>k</i> ≤ 14 –16 ≤ <i>l</i> ≤ 16
no. of collected rflns	7320
no. of unique rflns	6030
<i>R</i> _{int}	0.0310
no. of data (<i>I</i> > 4 σ (<i>I</i>))	3446
no. of params	362
goodness of fit	1.031
<i>R</i> 1/ <i>wR</i> 2 (<i>I</i> > 2 σ (<i>I</i>))	0.0623/0.1387
<i>R</i> 1/ <i>wR</i> 2 (all data)	0.1248/0.1653
min, max resd (e Å ⁻³)	–0.526, 0.485

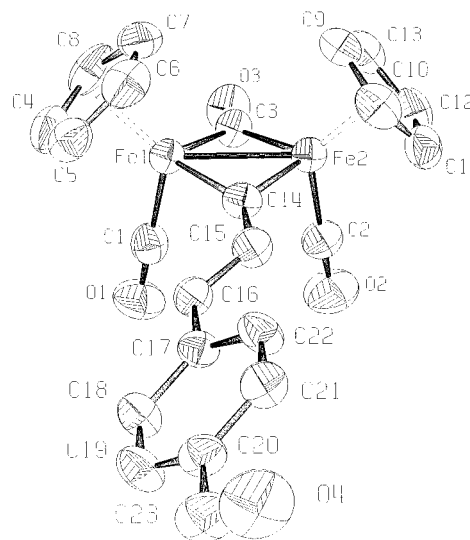
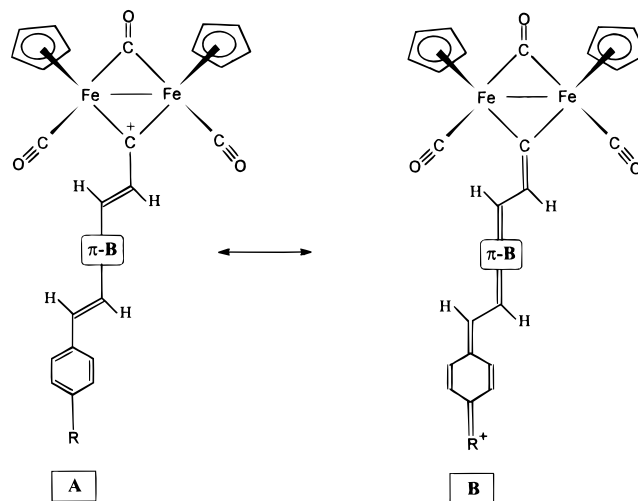
Table 2. Selected Bond Lengths (pm) and Angles (deg) for 17

Bond Lengths			
Fe(1)–C(1)	177.7(6)	C(14)–C(15)	142.8(7)
Fe(1)–C(3)	196.9(5)	C(15)–C(16)	135.1(7)
Fe(1)–C(14)	182.1(5)	C(16)–C(17)	147.0(7)
Fe(2)–C(2)	178.3(6)	C(17)–C(18)	139.4(7)
Fe(2)–C(3)	193.1(5)	C(18)–C(19)	138.5(8)
Fe(2)–C(14)	185.2(5)	C(19)–C(20)	136.8(8)
Fe(1)–Fe(2)	251.8(10)	C(20)–C(21)	138.5(8)
C(1)–O(1)	114.2(7)	C(20)–C(23)	148.9(8)
C(2)–O(2)	113.4(7)	C(21)–C(22)	138.9(7)
C(3)–O(3)	116.3(6)	C(22)–C(17)	138.5(7)
C(23)–O(4)	119.3(8)		
Bond Angles			
Fe(1)–[C4–C8] ^a	174.8(3)	C(16)–C(17)–C(18)	120.1(5)
Fe(2)–[C9–C13] ^b	174.8(3)	C(16)–C(17)–C(22)	120.8(5)
Fe(1)–C(3)–Fe(2)	80.4(2)	C(19)–C(20)–C(23)	121.2(5)
Fe(1)–C(14)–Fe(2)	86.6(2)	C(21)–C(20)–C(23)	119.0(5)
C(14)–C(15)–C(16)	123.1(5)	O(4)–C(23)–C(20)	124.5(6)
C(15)–C(16)–C(17)	124.7(5)		
Dihedral Angles			
[Fe(1)–C(3)–Fe(2)]/[Fe(1)–C(14)–Fe(2)] ^c	15.9(4)		
[Fe(1)–C(14)–Fe(2)]/[C(14)–C(16)]	21.6(9)		
[C(14)–C(17)]/[C(17)–C(22)] ^c	18.1(8)		
[C(20)–C(23)–O(4)]/[C(17)–C(22)] ^c	7.9(12)		

^a Center of the Cp ring C(4)–C(8). ^b Center of the Cp ring C(9)–C(13). ^c Angle between the two planes.

from planarity between the vinyl and aryl units may be as a consequence of poor communication between the aryl substituents.

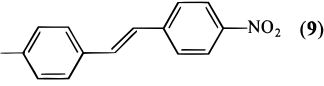
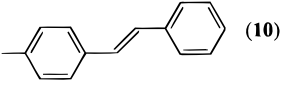
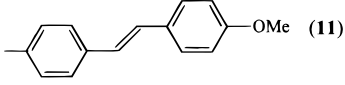
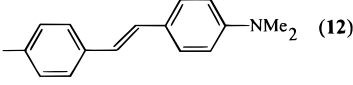
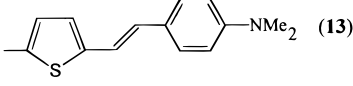
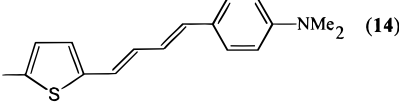
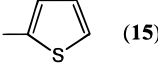
2.3. Structure of Complexes 9–14. The solution IR data of the complexes **9–14** (Table 3) reveal three bands in the carbonyl region similar to those for other reported cationic diiron vinylcarbyne complexes.^{11,14,15} The *cis* arrangement of the terminal carbonyl groups is established by the appearance of a strong band due to the symmetric stretch of the terminal CO ligands and a

**Figure 1.** Molecular structure of **17** (50% ellipsoids; hydrogens, solvent molecules, and BF₄ omitted for clarity).**Figure 2.** Limiting CT resonance forms for complexes **9–14**.

weak band of lower energy due to the asymmetric stretching vibration and is in agreement with the solid-state geometry discussed above. The broad, medium-intensity band at ca. 90 cm⁻¹ lower wavenumber is attributable to the stretching vibration of the bridging carbonyl ligand.

It is useful to consider the ground and excited states of these types of molecules as a combination of two limiting CT resonance forms (Figure 2). The shift to lower energy of the CO stretching modes in the order **9** < **10** < **11** < **12** (Table 3) reflects the π -donating properties of the bridging ligand and decreased positive charge localization at the Fe₂ terminus (type **A** resonance). As expected, the effect of minimizing the aromaticity of the bridging ligand on replacing a phenyl group by a thiophene unit led to more effective donor–acceptor ground-state communication with increased charge delocalization and greater M–CO back-donation. This indicates an increase in the contribution of the resonance form **B** to the ground state of these complexes.

Table 3. Solution IR and ^{13}C NMR Spectral Data for the Series $[(\text{CpFeCO})_2(\mu\text{-CO})(\mu\text{-CCH=CHD})][\text{BF}_4]$

D	IR (cm^{-1}) ^(a)		^{13}C NMR (ppm)
	$\nu(\text{CO})$	$\nu(\mu\text{-CO})$	$\mu\text{-C}$
 (9)	2037, 2006	1847	439 ^(b)
 (10)	2036, 2006	1847	438 ^(c)
 (11)	2036, 2005	1845	436 ^(c)
 (12)	2034, 2005	1844	432 ^(c)
 (13)	2027, 1998	1836	410 ^(c)
 (14)	2028, 1999	1838	412 ^(c)
 (15)	2035, 2005	1844	430 ^(c)

^a Solvent CH_2Cl_2 , ^b Solvent CDCl_3 , ^c Solvent CD_3CN .

The spectra also show the expected absorption bands due to the $[\text{BF}_4]^-$ ion and some unexpectedly strong bands lying between 1500 and 1600 cm^{-1} . Their intensities are comparable to those of the $\nu(\text{CO})$ modes: e.g. for **11** they are found at 1591 (4.2), 1558 (4.7), 1530 (9.7) and 1512 (10.3) cm^{-1} (relative intensities with $\nu(\text{CO})$ set to 10). As they are not present in the IR spectrum of **8**, they are attributed to the $\nu(\text{C}=\text{C})$ and other internal vibrations of the molecules. In contrast, in the IR spectra of the μ -alkenylidene complexes **18–20** these internal vibrations between 1500 and 1600 cm^{-1} are much weaker: e.g., for **19** one is found at 1514 (2.7) cm^{-1} .

Analyzing the ^1H and ^{13}C NMR spectra of compounds **9–14** provides further information about the ground-state structure of these chromophores. The nonequivalent cyclopentadienyl groups give rise to a single Cp resonance in the ^1H and ^{13}C NMR spectra at room temperature. This implies a rapid fluxional process such as rotation of the vinylcarbyne stilbene ligand, which exchanges the environment of the two Cp ligands in solution. The same is not true for **18–20**, where two such resonances are observed, consistent with the fixed $\mu\text{-C}=\text{C}$ double bond of the μ -alkenylidene ligand. Fenske–Hall molecular orbital calculations on these types

of μ -vinylcarbyne complexes reveal that the perpendicular π -orbitals of the $\mu\text{-C}$ can accept electron density throughout rotation of the $\mu\text{-C}$ vinyl ligand and thus facilitate rotation of the ligand without diminishing electronic interaction.⁶

The chemical shift of the $\mu\text{-C}$ in the ^{13}C NMR spectra of dinuclear carbonyl complexes with bridging vinylidyne ligands is an excellent diagnostic for the extent of charge delocalization in the ground state. The greater the extent of charge delocalization, the greater the upfield shift of the $\mu\text{-C}$ signal. First, comparing the $\mu\text{-C}$ signal of the vinylidyne complex **9** (Table 3) with that of the complex $[(\text{CpFeCO})_2(\mu\text{-CO})(\mu\text{-CCH}=\text{C}(\text{CH}_3)_2)][\text{BF}_4]$ ¹⁶ (δ 440 ppm) demonstrates that for **9** it is essentially the vinyl group which effects delocalization and confirms the dominant contribution of an A-type resonance structure to the ground state of **9**. However, the respective shielding of the $\mu\text{-C}$ ^{13}C NMR signals of the complexes **10–14** concurs with the trend in the IR data, that the ground state for these complexes has increased contribution from the quinone-type resonance **B** in accordance with the electron-donating ability of the

(16) Casey, C. P.; Miles, W. H.; Tukada, H. *J. Am. Chem. Soc.* **1985**, *107*, 2924.

Table 4. Optical Data for the Series 9–14

compd	λ_{\max} (ϵ M ⁻¹ cm ⁻¹) nm		$\Delta\nu$ (cm ⁻¹) ^a	β^b (10 ⁻³⁰ esu)	β_0 (10 ⁻³⁰ esu)
	CH ₂ Cl ₂	CH ₃ CN			
9	463 (40 326)	437 (34 313)	-1285	346 ^e	68
10	513 (57 898)	481 (44 344)	-1297	792	43
11	553 (46 240)	512 (47 356)	-1448		
12	686 (39 517)	602 (34 181)	-2034	^c	
13	765 (62 254)	696 (49 517)	-1296	2443 ^e 1623 ^{d,e}	1260 661
14	795 (50 705)	693 (44 535)	-1851		

^a $\Delta\nu = (\nu_{\max} \text{ in CH}_2\text{Cl}_2) - (\nu_{\max} \text{ in CH}_3\text{CN})$. ^b Measured in CH₂Cl₂ with reference *p*-NA ($\beta = 21.6 \times 10^{-30}$ esu). ^c Not measurable. ^d Measured in CH₃CN with reference *p*-NA ($\beta = 29.2 \times 10^{-30}$ esu). ^e Fluorescence enhanced.

para substituent. Nonetheless, it must be noted that the ground-state structures of **9–14** are still fundamentally structure **A** based (Figure 2).

As expected, the reduced aromaticity of thiophene as compared to benzene (stabilization energy: thiophene is 29 kcal mol⁻¹ versus 36 kcal mol⁻¹ for benzene) facilitates better electron delocalization. This is reflected in a 22 ppm upfield shift in the μ -C signal of **13** relative to **12**. However, it is possible that the thiophene group itself in **13** is acting as an additional donor within the bridge. To investigate this effect, thiophene-2-carbaldehyde was reacted with [(CpFeCO)₂(μ -CO)(μ -CCH₃)]-[BF₄]₂ (**8**) and the relevant spectroscopic details are presented in Table 3. The data demonstrate that, when it is coupled to the cationic diiron (CpFeCO)₂(μ -CO)(μ -CCH=CH-) electron acceptor unit, thiophene allows ground-state delocalization comparable to that of the (dimethylamino)stilbene ligand in **12**. Nonetheless, in a comparison of the spectral characteristics of **12** and **13**, the effect is such that it is best to consider the thiophene moiety as an auxiliary donor within the bridge.

2.4. Electronic Absorption Spectra. The optical absorption data for the series **9–14** are presented in Table 4. The low-energy band observed in the UV-vis spectra of **9–14** is attributed to a donor-acceptor based charge transfer upon photochemical excitation. The series exhibits large negative solvatochromism of this CT band. If we consider that in the ground state the positive charge is essentially localized on the Fe₂(μ -C) acceptor center as indicated by IR and NMR spectroscopy, then upon excitation some of the electron density from the electron-donating stilbenyl substituent may be shifted to the acceptor. As a result, the positive charge will be more equally distributed on both termini of the molecule, resulting in a less polar molecule upon excitation. Thus, we find that a polar solvent lowers the energy of the ground state more than that of the excited state, leading to the observed negative solvatochromism. The increase of the solvatochromic effect corresponds to an increase in the change in dipole moment between the ground and excited states. Complex **12** exhibits the largest negative solvatochromism (-2034 cm⁻¹), implying that in the series **9–14** it has the largest dipole moment difference between the ground and excited states.

As a function of increasing donor strength the UV-vis absorption spectra of **9–14** display significant bathochromic shifts (Figure 3), which is further evidence for the strong contribution of resonance **B** to the excited state. Increasing the donor strength of the ligand has

the effect of stabilizing the charge delocalized excited state, resulting in a lower energy CT band. Comparing the electronic absorption spectra of **12** and **13** reveals that replacement of the phenyl ring by a thienyl unit also causes a bathochromic shift of the CT band by 1505 cm⁻¹. Moreover, **13** exhibits less solvatochromism than **12** and this may be regarded as a consequence of the greater charge delocalization over the thienyl unit in the ground state, resulting in a lower dipole moment difference upon excitation. As anticipated, elongation of the conjugating bridge (complex **14**) results in a decrease in the energy of the charge-transfer band.

2.5. Hyperpolarizability Measurements. Previous studies of organometallic cyanines containing the (CpFeCO)₂(μ -CO)(μ -C) fragment are few, but they have established the potential of incorporating this moiety into NLO candidates. A series of complexes of the form [(CpFeCO)₂(μ -CO)(μ -CR)][X] were examined by the Kurtz powder technique using $\omega = 1907$ nm incident radiation.²² The best result was found in the case where R = -CH=CHC₆H₄-*p*-NMe₂ and X = CF₃SO₃, which exhibited a second harmonic signal 3.6 times that of a urea reference standard. However, powder testing results are dependent on criteria such as particle size, solvent of crystallization, and favorable orientation of molecular dipoles in the crystal lattice and as such are not reliable sources of information about molecular hyperpolarizabilities.¹⁸ The optical properties of another series of merocyanine chromophores possessing the (CpFeCO)₂(μ -CO)(μ -C=CH-) unit as an electron donor and thiobarbituric acid as the electron acceptor linked with one to three double bonds also demonstrated the potential of these metal-in-plane organometallic termini.¹⁹ The larger $\mu\beta_0$ values (a dot product of the dipole moment and the static first hyperpolarizability) obtained relative to the organic trimethylindoline donor based analogues demonstrated the effective electron-donating capabilities of the organometallic moiety.

Care should be taken when comparing the NLO values obtained from different techniques due to variations in the measurement conditions and mechanisms. Recently, some of the problems in comparing electric field induced second-harmonic generation (EFISH) and hyper-Rayleigh scattering (HRS) data as well as the results obtained at different wavelengths have been documented.²⁰ As the NLO properties of the chromophores in this work were examined by the HRS technique, no comparisons will be drawn between them and the diiron series mentioned above.

The first hyperpolarizabilities β of the complexes **9**, **10**, **12**, and **13** are presented in Table 4. HRS experiments were not carried out on the complexes **11** and **14**, as they possess strong absorption bands in the areas of either the fundamental or second-harmonic generated (SHG) signals. The HRS experiments were

(17) Bandy, J. A.; Bunting, H. E.; Garcia, M.-H.; Green, M. L. H.; Marder, S. R.; Thompson, M. E. *Polyhedron* **1992**, *12*, 1429.

(18) Perry, J. W. *ACS Symp. Ser.* **1991**, No. 455, 71.

(19) Zu, W.; Ortiz, R.; Fort, A.; Barzoukas, M.; Marder, S. R. *J. Organomet. Chem.* **1997**, *528*, 217.

(20) (a) Clays, K.; Hendrickx, E.; Verbiest, T.; Persoons, A. *Adv. Mater.* **1998**, *10*, 643. (b) Wolff, J. J.; Wortmann, R. *J. Prakt. Chem.* **1998**, *340*, 99.

(21) Clays, K.; Persoons, A. *Rev. Sci. Instrum.* **1992**, *63*, 3285.

(22) (a) Oudar, J. L.; Chemla, D. S. *Chem. Phys.* **1977**, *66*, 2664. (b) Hendrickx, E.; Clays, K.; Persoons, A.; Dehu, C.; Bredas, J. L. *J. Am. Chem. Soc.* **1995**, *363*, 58.

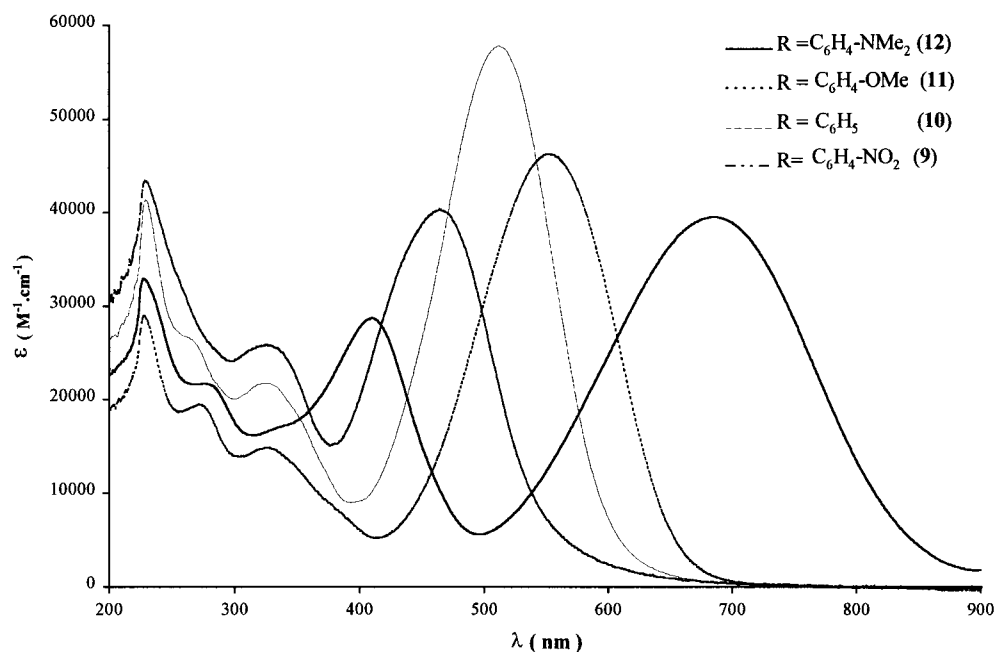


Figure 3. Electronic absorption spectra of the series $[(\text{CpFeCO})_2(\mu\text{-CO})(\mu\text{-CCH=CHC}_6\text{H}_4\text{CH=CHR})][\text{BF}_4]$.

carried out in dichloromethane and acetonitrile solutions at 1064 nm fundamental wavelength. The β values of the compounds are resonance-enhanced, and therefore, the static first hyperpolarizabilities (β_0) have been calculated using the two-level model.²² During the HRS experiment a dissolved sample of the NLO chromophore is irradiated with a laser beam of intensity $I(\omega)$, and the intensity of the frequency-doubled scattered light $I(2\omega)$ is recorded as a function of $I(\omega)$. The dependence of the ratio $I(2\omega)/I(\omega)^2$ from the concentration of the NLO chromophore referred against a standard leads to the $\beta(\text{HRS})$ value.²¹ Measurement of β for compound **12** was not possible, as the relationship between the intensities of the fundamental and the frequency-doubled light was not quadratic.

The β_0 values obtained are of such magnitude that a check for multiphoton-induced fluorescence enhancement was undertaken. This was achieved using band-pass filters at λ 400, 450, 500, 532, 560, 650, and 700 nm with a bandwidth of 10 nm as reported earlier.²³ A reasonable fluorescence contribution was found for the complexes **9** and **13** (Figure 4). However, the emission spectra of **10** and **12** reveal no fluorescence near the HRS signal (Figure 5). Another indication of the fluorescence enhancement is the halving of the β_0 values on changing solvents for **13**. Nonetheless, the β_0 value for **9** is quite high and demonstrates the high polarizability of hydrocarbon bridges and the amphoteric nature of the nitro group in donor–acceptor systems.

3. Conclusion

In this paper we have synthesized a series of μ -alkenylidene complexes by two complementary procedures. The concept of using the $[(\text{CpFeCO})_2(\mu\text{-CO})(\mu\text{-CCH=CH-})]^+$ ionic fragment as an electron acceptor was rewarded by the high β values obtained, although fluorescence checks reveal that in some cases calculation of β_0 from these values may include a significant enhancement due to two-photon absorption fluorescence

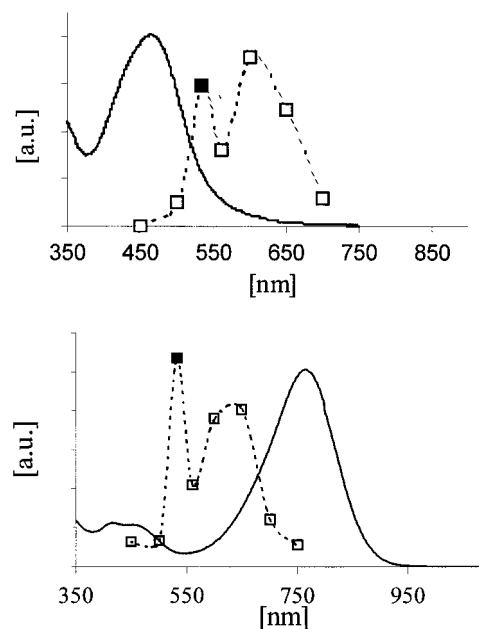


Figure 4. Absorption (solid line) and emission spectra (dotted line) of complexes **9** (top) and **13** (bottom) in CH_2Cl_2 . The filled square is the λ 532 nm signal.

(TPAF). On the other hand, several applications of two-photon excitation have been reported, and hence, these chromophores may also have some potential in these areas.²⁴

Further series of complexes linking this acceptor unit to polyaromatic and organometallic donors have been produced and will be the subject of future publications. Initial investigations of their second-order optical non-

(23) Wong, H.; Meyer-Friedrichsen, T.; Farrell, T.; Mecker, C.; Heck, J. *Eur. J. Inorg. Chem.* **2000**, 4, 631.

(24) (a) Parthenopoulos, D. M.; Rentzepis, P. M. *Science* **1989**, 24, 843. (b) Cumpston, B. H.; Ananthavel, S. P.; Barlow, S.; Dyer, D. L.; Ehrlich, J. E.; Erskine, L. L.; Heikal, A. A.; Kuebler, S. M.; Sandy Lee, I.-Y.; McCord-Maughon, D.; Qin, J.; Röckel, H.; Rumi, M.; Wu, X.-L.; Marder, S. R.; Perry, J. W. *Nature* **1999**, 398, 51.

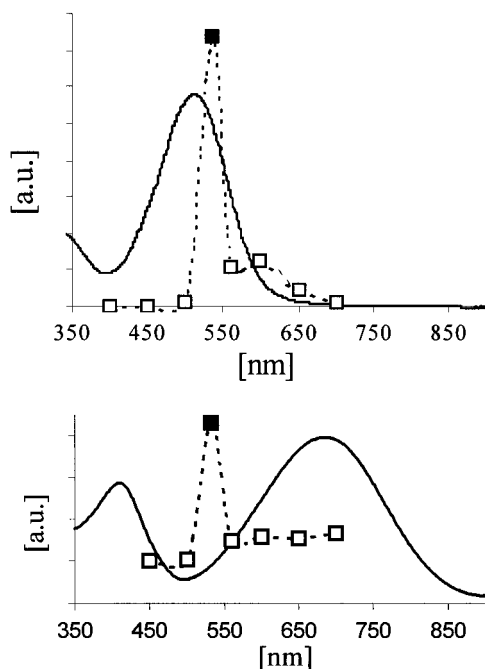


Figure 5. Absorption (solid line) and emission spectra (dotted line) of complex **10** (top) and **12** (bottom) in CH_2Cl_2 . The filled square is the λ 532 nm signal.

linearities are also interesting. Moreover, it is hoped that by using longer incident wavelengths for HRS measurements and a monochromator to obtain the nonlinear emission spectra, the problem of β_0 overestimation due to TPFA can be overcome.

4. Experimental Section

Dichloromethane and THF were dried by refluxing over calcium hydride and distilled prior to use. THF was further distilled from sodium–benzophenone. Acetonitrile was dried by refluxing over calcium sulfate and distilled prior to use. Chromatography was carried out on aluminum oxide (Merck: 101097), unless otherwise stated. Infrared spectra were recorded on a Perkin-Elmer Paragon 1000 spectrometer. UV–vis spectra were recorded on a Perkin-Elmer Lambda 6 spectrometer. NMR spectra were recorded on a JEOL JNM-GX 270 FT spectrometer using TMS as an internal standard. Elemental analysis was carried out by the Microanalytical Laboratory, University College, Dublin, Ireland.

4.1. General Procedure for the Condensation of [(Cp-FeCO) $_2(\mu\text{-CO})(\mu\text{-CCH=CH})$][BF $_4$] (8**) with Aldehydes.** Complex **8** (0.5 g, 1.14 mmol) and an excess of the aldehyde (1.3 mmol) were stirred in CH_2Cl_2 (50 cm^3) at 35 $^\circ\text{C}$ for 12 h. The reaction mixture was filtered and the product precipitated from the filtrate by carefully adding diethyl ether (25 cm^3) and cooling overnight.

9. Yield: 0.39 g (51%). ^1H NMR (CDCl_3): δ 9.80 (d, 1H, J = 14.9 Hz, $\mu\text{-CCH=CH}$), 8.11 (d, 2H, J = 9.0 Hz, C_6H_4), 8.00 (d, 2H, J = 8.2 Hz, C_6H_4), 7.52 (d, 1H, J = 14.9 Hz, $\mu\text{-CCH=CH}$), 7.40 (d, 2H, J = 9.0 Hz, C_6H_4), 7.35 (d, 2H, J = 8.2 Hz, C_6H_4), 6.81 (s, 2H, $\text{C}_6\text{H}_4\text{CH=CH}$), 5.32 (s, 10H, C_5H_5) ppm. ^{13}C NMR (CDCl_3): δ 439.42 ($\mu\text{-C}$), 253.4 ($\mu\text{-CO}$), 206.84 (CO), 151.98, 150.08 ($\mu\text{-CCH=CH}$), 146.92, 143.47, 142.14, 133.35 (C_q C_6H_4), 132.62, 130.40, 129.77, 123.85 (C_6H_4), 132.71, 130.85 ($\text{C}_6\text{H}_4\text{CH=CH}$), 91.74 (C_5H_5) ppm. IR (CH_2Cl_2): ν_{CO} 2037 (vs), 2006 (m), 1847 (s); $\nu_{\text{C=C}}$ 1596 (m), 1561 (s), 1535 (vs), 1516 (s) cm^{-1} . UV–vis (CH_2Cl_2): λ_{max} (ϵ) 463 nm (40 326 $\text{M}^{-1} \text{cm}^{-1}$). UV–vis (CH_3CN): λ_{max} (ϵ) 437 nm (34 313 $\text{M}^{-1} \text{cm}^{-1}$). Anal. Calcd for $\text{C}_{30}\text{H}_{22}\text{Fe}_2\text{NO}_3\text{BF}_4 \cdot 1/2\text{H}_2\text{O}$: C, 53.38 (52.55); H, 3.29 (3.36); N, 2.08 (2.04). Found: C, 52.22; H, 3.19; N, 2.02%.

10. Yield: 0.47 g (66%). ^1H NMR (CD_3CN): δ 10.44 (d, 1H, J = 14.9 Hz, $\mu\text{-CCH=CH}$), 8.48 (d, 2H, J = 8.2 Hz, C_6H_4), 8.25 (d, 1H, J = 14.9 Hz, $\mu\text{-CCH=CH}$), 8.04 (d, 2H, J = 8.2 Hz, C_6H_4), 7.78 (d, 1H, J = 16.3 Hz, $\text{C}_6\text{H}_4\text{CH=CH}$), 7.57 (d, 2H, J = 7.3 Hz, C_6H_5), 7.30 (m, 4H, $p\text{-C}_6\text{H}_5$, C_6H_4 , $\text{C}_6\text{H}_4\text{CH=CH}$), 5.83 (s, 10H, C_5H_5) ppm. ^{13}C NMR (CD_3CN): δ 438.32 ($\mu\text{-C}$), 255.25 ($\mu\text{-CO}$), 208.99 (CO), 152.58, 152.39 ($\mu\text{-CCH=CH}$), 144.8, 138.06, 134.65 (C_q C_6H_4 , C_q C_6H_5), 134.08, 130.22, 129.08, 128.29 ($o,m\text{-C}_6\text{H}_4$, $o,m\text{-C}_6\text{H}_5$), 133.94 ($p\text{-C}_6\text{H}_5$), 129.96, 128.79 ($\text{C}_6\text{H}_4\text{CH=CH}$), 93.14 (C_5H_5) ppm. IR (CH_2Cl_2): ν_{CO} 2036 (vs), 2007 (m), 1846 (s); $\nu_{\text{C=C}}$ 1600 (s), 1560 (s), 1532 (vs), 1506 (s) cm^{-1} . UV–vis (CH_2Cl_2): λ_{max} (ϵ) 513 nm (57 898 $\text{M}^{-1} \text{cm}^{-1}$). UV–vis (CH_3CN): λ_{max} (ϵ) 481 nm (44 344 $\text{M}^{-1} \text{cm}^{-1}$). Anal. Calcd for $\text{C}_{30}\text{H}_{23}\text{Fe}_2\text{O}_3\text{BF}_4 \cdot 1/2\text{CH}_2\text{Cl}_2$: C, 57.19 (54.42); H, 3.68 (3.57). Found: C, 54.55; H, 3.52.

11. Yield: 0.50 g (67%). ^1H NMR ($(\text{CD}_3)_2\text{CO}$): δ 10.29 (d, 1H, J = 14.9 Hz, $\mu\text{-CCH=CH}$), 8.31 (d, 2H, J = 8.2 Hz, C_6H_4), 8.11 (d, 1H, J = 14.9 Hz, $\mu\text{-CCH=CH}$), 7.86 (d, 2H, J = 8.2 Hz, C_6H_4), 7.67 (d, 2H, J = 8.4 Hz, C_6H_4), 7.60 (d, 1H, J = 16.6 Hz, $\text{C}_6\text{H}_4\text{CH=CH}$), 7.28 (d, 1H, J = 16.6 Hz, $\text{C}_6\text{H}_4\text{CH=CH}$), 7.01 (d, 2H, J = 8.4 Hz, C_6H_4), 5.69 (s, 10H, C_5H_5), 3.86 (s, 3H, OMe) ppm. ^{13}C NMR (CD_3CN): δ 435.94 ($\mu\text{-C}$), 254.64 ($\mu\text{-CO}$), 208.32 (CO), 160.90, 144.83, 133.41, 129.99 (C_q C_6H_4), 152.33, 151.50 ($\mu\text{-CCH=CH}$), 133.50, 129.14, 128.06, 114.93 ($o,m\text{-C}_6\text{H}_4$), 133.19, 125.78 ($\text{C}_6\text{H}_4\text{CH=CH}$), 92.38 (C_5H_5), 55.62 (OMe) ppm. IR (CH_2Cl_2): ν_{CO} 2036 (vs), 2005 (m), 1845 (s); $\nu_{\text{C=C}}$ 1591 (s), 1558 (s), 1530 (vs), 1512 (vs) cm^{-1} . UV–vis (CH_2Cl_2): λ_{max} (ϵ) = 553 nm (46 240 $\text{M}^{-1} \text{cm}^{-1}$). UV–vis (CH_3CN): λ_{max} (ϵ) 512 nm (47 536 $\text{M}^{-1} \text{cm}^{-1}$). Anal. Calcd for $\text{C}_{31}\text{H}_{23}\text{Fe}_2\text{O}_4\text{BF}_4 \cdot \text{CH}_2\text{Cl}_2$: C, 56.36 (51.54); H, 3.79 (3.62). Found: C, 51.84; H, 3.75.

12. Yield: 0.43 g (56%). ^1H NMR (CD_3CN): δ 10.27 (d, 1H, J = 14.6 Hz, $\mu\text{-CCH=CH}$), 8.28 (d, 2H, J = 7.6 Hz, C_6H_4), 8.10 (d, 1H, J = 14.6 Hz, $\mu\text{-CCH=CH}$), 7.83 (d, 2H, J = 8.2 Hz, C_6H_4), 7.60 (d, 2H, J = 7.6 Hz, C_6H_4), 7.50 (hidden, $\text{C}_6\text{H}_4\text{CH=CH}$), 7.19 (d, 1H, J = 16.0 Hz, $\text{C}_6\text{H}_4\text{CH=CH}$), 6.88 (d, 2H, J = 8.2 Hz, C_6H_4), 5.68 (s, 10H, C_5H_5), 3.08 (s, 6H, NMe $_2$) ppm. ^{13}C NMR (CD_3CN): δ 432.43 ($\mu\text{-C}$), 255.08 ($\mu\text{-CO}$), 208.48 (CO), 153.05, 151.22 ($\mu\text{-CCH=CH}$), 146.0, 132.71, 130.59, 125.25 (C_q C_6H_4), 133.79, 129.23, 127.75, 112.94 ($o,m\text{-C}_6\text{H}_4$), 134.58, 123.13, ($\text{C}_6\text{H}_4\text{CH=CH}$), 92.34 (C_5H_5), 40.15 (N(CH $_3$) $_2$) ppm. IR (CH_2Cl_2): ν_{CO} 2034 (vs), 2005 (m), 1844 (s); $\nu_{\text{C=C}}$ 1584 (vs), 1557 (vs), 1520 (vs), 1498 (vs) cm^{-1} . UV–vis (CH_2Cl_2): λ_{max} (ϵ) = 686 nm (39 517 $\text{M}^{-1} \text{cm}^{-1}$). UV–vis (CH_3CN): λ_{max} (ϵ) 602 nm (34 181 $\text{M}^{-1} \text{cm}^{-1}$). Anal. Calcd for $\text{C}_{32}\text{H}_{22}\text{Fe}_2\text{NO}_3\text{BF}_4$: C, 57.1; H, 4.19; N, 2.08. Found: C, 58.55; H, 4.70; N, 2.67.

13. Yield: 0.38 g (49%). ^1H NMR (CD_3CN): δ 9.51 (d, 1H, J = 13.8 Hz, $\mu\text{-CCH=CH}$), 8.19 (d, 1H, J = 4.2 Hz, th), 8.02 (d, 1H, J = 13.8 Hz, $\mu\text{-CCH=CH}$), 7.64 (d, 2H, J = 8.7 Hz, $o,m\text{-C}_6\text{H}_4$), 7.52 (d, 1H, J = 16.0 Hz, (th)CH=CH), 7.47 (hidden, th), 7.39 (d, 1H, J = 16.0 Hz, (th)CH=CH), 6.91 (d, 2H, J = 8.7 Hz, $o,m\text{-C}_6\text{H}_4$), 5.38 (s, 10H, C_5H_5), 3.11 (s, 6H, NMe $_2$) ppm. ^{13}C NMR (CD_3CN): δ 408.67 ($\mu\text{-C}$), 257.14 ($\mu\text{-CO}$), 209.08 (CO), 162.32, 152.41, 137.46, 124.01 (C_q C_6H_4 , C_q th), 149.0, 146.28, 138.19, 130.21, 129.74, 117.24, 116.64, 112.81 ($\mu\text{-CCH=CH}$; $o,m\text{-C}_6\text{H}_4$; C3, C4 th; (th)CH=CH), 91.71 (C_5H_5), 39.99 (–NMe $_2$) ppm. IR (CH_2Cl_2): ν_{CO} 2027 (vs), 1998 (m), 18.36 (s); $\nu_{\text{C=C}}$ 1586 (vs), 1519 (vs), 1490 (s) cm^{-1} . UV–vis (CH_2Cl_2): λ_{max} (ϵ) = 765 nm (62 254 $\text{M}^{-1} \text{cm}^{-1}$). UV–vis (CH_3CN): λ_{max} (ϵ) 696 nm (49 517 $\text{M}^{-1} \text{cm}^{-1}$). Anal. Calcd for $\text{C}_{30}\text{H}_{26}\text{Fe}_2\text{O}_3\text{NSBF}_4 \cdot 1/2\text{H}_2\text{O}$: C, 53.02 (52.33); H, 3.83 (3.92); N, 2.06 (2.03). Found: C, 52.32; H, 3.51; N, 1.99.

14. Yield: 0.31 g (39%). ^1H NMR (CD_3CN): δ 9.46 (d, 1H, J = 13.8 Hz, $\mu\text{-CCH=CH}$), 8.11 (s, 1H, th), 7.95 (d, 1H, J = 13.8 Hz, $\mu\text{-CCH=CH}$), 7.46 (d, 2H, J = 8.7 Hz, $o,m\text{-C}_6\text{H}_4$), 7.37 (2H, br), 6.96 (3H, br), 6.89 (2H, br), 5.33 (s, 10H, C_5H_5), 3.01 (s, 6H, NMe $_2$) ppm. ^{13}C NMR (CD_3CN): δ 412.37 ($\mu\text{-C}$), 256.79 ($\mu\text{-CO}$), 208.95 (CO), 160.39, 151.25, 138.31, 126.13 (C_q C_6H_4 ; C_q th), 149.29, 145.84, 145.27, 140.15, 138.85, 130.31, 129.39, 124.77, 122.81, 111.32 ($\mu\text{-CCH=CH}$; C3, C4 th; (th)CH=CH, CH=CHC $_6\text{H}_5$; $o,m\text{-C}_6\text{H}_4$), 91.81 (C_5H_5), 40.49 (NMe $_2$) ppm. IR

(CH₂Cl₂): ν_{CO} 2029 (vs), 1999 (m), 1838 (s); $\nu_{\text{C}=\text{C}}$ 1612 (m), 1598 (m), 1525 (m), 1489 (s) cm⁻¹. UV-vis (CH₂Cl₂): λ_{max} (ϵ) = 795 nm (50 705 M⁻¹ cm⁻¹). UV-vis (CH₃CN): λ_{max} (ϵ) 693 nm (44 535 M⁻¹ cm⁻¹). Anal. Calcd for C₃₂H₂₈Fe₂O₃NSBF₄·H₂O: C, 54.47 (53.11); H, 3.97 (4.15); N, 1.99 (1.94). Found: C, 53.13; H, 4.43; N, 1.97.

15. Yield: 0.41 g (68%). ¹H NMR (CD₃CN): δ 9.66 (d, 1H, J = 14.6 Hz, μ -CCH=CH), 8.25 (d, 1H, J = 4.8 Hz, H⁵ C₄H₄S), 8.22 (d, 1H, J = 3.9 Hz, H³ C₄H₄S), 8.05 (d, 1H, J = 14.6 Hz, μ -CCH=CH), 7.42 (dd, 1H, J = 4.8, 3.9 Hz, H⁴ C₄H₄S), 5.38 (s, 10H, C₅H₅) ppm. ¹³C NMR (CD₃CN): δ 430.20 (μ -C), 254.93 (μ -CO), 208.40 (CO), 150.66, 145.54 (μ -CCH=CH), 140.37 (C_q C₄H₄S), 141.70 (C³ C₄H₄S), 139.94 (C⁵ C₄H₄S), 131.58 (C⁴ C₄H₄S), 92.28 (C₅H₅) ppm. IR (CH₂Cl₂): ν_{CO} 2035 (vs), 2005 (m), 1844 (s); $\nu_{\text{C}=\text{C}}$ 1540 (vs), 1497 (w) cm⁻¹. UV-vis (CH₂Cl₂): λ_{max} (ϵ) = 460 nm (25 650 M⁻¹ cm⁻¹). UV-vis (CH₃CN): λ_{max} (ϵ) 449 nm (23 599 M⁻¹ cm⁻¹). Anal. Calcd for C₂₀H₁₅Fe₂O₃·SBF₄: C, 44.94; H, 2.81. Found: C, 44.80; H, 2.96.

4.2. Condensation of [(CpFeCO)₂(μ -CO)(μ -CCH₃)] [BF₄] (8**) with Terephthalaldehyde.** Complex **8** (0.5 g, 1.14 mmol) was stirred in CH₂Cl₂ (50 cm³) with terephthalaldehyde (0.24 g, 1.15 mmol) at 35 °C for 12 h. The reaction mixture was filtered and the precipitate analyzed as [(CpFeCO)₂(μ -CO)(μ -CCH=CHC₆H₄CH=CHC)(μ -CO)(CpFeCO)₂] [BF₄]₂ (**16**) (0.3 g, 34%). The filtrate was reduced in volume and cooled overnight. A microcrystalline solid was obtained on filtration and was characterized as [(CpFeCO)₂(μ -CO)(μ -CCH=CHC₆H₄CHO)] (**17**; 0.32 g, 52%).

16. ¹H NMR (CDCl₃): δ 10.01 (d, 1H, J = 14.9 Hz, μ -CCH=CH), 8.36 (s, 4H, C₆H₄), 7.74 (d, 1H, J = 14.9 Hz, μ -CCH=CH), 5.46 (s, 10H, C₅H₅) ppm. IR (CH₃CN): ν_{CO} 2039 (vs), 2005 (m), 1848 (s) cm⁻¹. Anal. Calcd for C₃₈H₂₈Fe₄O₆(BF₄)₂·0.2CH₂Cl₂: C, 46.63 (41.81); H, 2.86 (2.79). Found: C, 41.77; H, 2.93.

17. ¹H NMR (CD₃CN): δ 10.19 (s, 1H, CHO), 10.01 (d, 1H, J = 15.2 Hz, μ -CCH=CH), 8.40 (d, 2H, J = 8.2 Hz, C₆H₄), 8.17 (d, 2H, J = 8.2 Hz, C₆H₄), 7.78 (d, 1H, J = 15.2 Hz, μ -CCH=CH), 5.50 (s, 10H, C₅H₅) ppm. ¹³C NMR (CD₃CN): δ 447.24 (μ -C), 253.40 (μ -CO), 208.20 (CO), 193.16 (CHO), 153.71, 147.26 (μ -CCH=CH), 140.61, 139.61 (C_q C₆H₄), 132.71, 131.15 (*o,m*-C₆H₄), 93.15 (C₅H₅) ppm. IR (CH₂Cl₂): ν_{CO} 2040 (vs), 2008 (m), 1850 (s); ν_{CHO} 1703 (s); $\nu_{\text{C}=\text{C}}$ 1577 (m), 1549 (s) cm⁻¹. Anal. Calcd for C₂₃H₁₇Fe₂O₄BF₄: C, 49.64; H, 3.06. Found: C, 49.31; H, 3.20.

4.3. Reaction of [(CpFeCO)₂(μ -CO)(μ -CCH=CHC₆H₄CHO)] [BF₄] (17**) with [Et₄N][HFe(CO)₄].** [Et₄N][HFe(CO)₄]¹² (0.54 g, 1.81 mmol) was added to a solution of **17** (0.5 g, 0.9 mmol) in THF (75 cm³). A red solution was formed, and stirring was continued for 1 h. The reaction mixture was filtered and the volume reduced. The residue was extracted with ether, the extracts were dried over MgSO₄, and the solvent was removed. Chromatography with CH₂Cl₂ on alumina followed by recrystallization from CH₂Cl₂/hexane yielded [(CpFeCO)₂(μ -CO)(μ -C=CHCH₂C₆H₄CHO)] (**18**; 0.32 g, 76%).

¹H NMR (CDCl₃): δ 9.99 (s, 1H, C₆H₄CHO), 7.86 (d, 2H, J = 8.2 Hz, C₆H₄), 7.59 (d, 2H, J = 8.2 Hz, C₆H₄), 7.22 (t, 1H, J = 7.0 Hz, μ -C=CH), 4.84 (s, C₅H₅), 4.80 (s, C₅H₅), 4.21 (m, 2H, μ -C=CHCH₂) ppm. ¹³C NMR (CDCl₃): δ 271.55 (μ -C), 267.88 (μ -CO), 210.97 (CO), 192.07 (C₆H₄CHO), 137.06 (μ -C=CH), 150.63, 134.37 (C_q C₆H₄), 130.0, 128.82 (*o,m*-C₆H₄), 87.62, 86.86 (C₅H₅), 43.45 (μ -C=CHCH₂) ppm. IR (CH₂Cl₂): ν_{CO} 1992 (vs), 1954 (m), 1788 (s); ν_{CHO} 1697 (s) cm⁻¹. Anal. Calcd for C₂₃H₁₈Fe₂O₄: C, 58.71; H, 3.83. Found: C, 58.60; H, 3.91.

4.4. General Procedure for the Reaction of [(CpFeCO)₂(μ -CO)(μ -C=CHCH₂C₆H₄CHO)] (18**) with [RCH₂PPh₃]₂ [X] (R = 4-OMeC₆H₄-, 4-Me₂NC₆H₄-).** A solution of [RCH₂PPh₃]₂ [X] and *t*-BuOK (1.1 equiv) was stirred in dry THF for 1 h. **18** (0.3 g, 1.1 mmol) was added and stirring continued for 3 h. The reaction mixture was filtered through MgSO₄, and the solvent was removed. The residue was taken up in CH₂Cl₂ and chromatographed on alumina. Products were eluted with CH₂Cl₂ and were recrystallized from CH₂Cl₂/hexane.

19. Yield: 0.26 g (72%). ¹H NMR (CDCl₃): δ 7.44 (m, 6H, C₆H₄), 7.25 (t, 1H, J = 7.0 Hz, μ -C=CH), 7.06 (d, 1H, J = 16.3 Hz, C₆H₄CH=CH), 6.97 (d, 1H, J = 16.3 Hz, C₆H₄CH=CH), 6.89 (d, 2H, J = 8.8 Hz, C₆H₄), 4.83 (s, C₅H₅), 4.78 (s, C₅H₅), 4.13 (d, 2H, J = 7.0 Hz, μ -C=CHCH₂), 3.83 (s, 3H, OMe) ppm. ¹³C NMR (CDCl₃): δ 272.47 (μ -CO), 266.90 (μ -C), 210.99 (CO), 159.11, 142.30, 135.27, 130.33 (C_q C₆H₄), 138.56 (μ -C=CH), 128.54, 127.57, 126.36, 114.09 (*o,m*-C₆H₄), 127.32, 126.56 (C₆H₄CH=CH), 87.64, 86.91 (C₅H₅), 55.313 (OMe), 43.02 (μ -C=CHCH₂) ppm. IR (CH₂Cl₂): ν_{CO} 1991 (vs), 1953 (m), 1786 (s); $\nu_{\text{C}=\text{C}}$ 1514 (m) cm⁻¹. Anal. Calcd for C₃₁H₂₆Fe₂O₄: C, 64.81; H, 4.53. Found: C, 64.95; H, 4.57.

20. Yield: 0.30 g (79%). ¹H NMR (CDCl₃): δ 7.44 (m, 6H, C₆H₄), 7.26 (t, 1H, J = 7.1 Hz, μ -C=CH), 7.04 (d, 1H, J = 16.3 Hz, C₆H₄CH=CH), 6.92 (d, 1H, J = 16.3 Hz, C₆H₄CH=CH), 6.72 (d, 2H, J = 8.8 Hz, C₆H₄), 4.83 (s, C₅H₅), 4.79 (s, C₅H₅), 4.20 (d, 2H, J = 7.2 Hz, μ -C=CHCH₂), 2.97 (s, 6H, NMe₂) ppm. ¹³C NMR (CDCl₃): δ 272.61 (μ -C), 266.82 (μ -CO), 211.01 (CO), 150.02, 141.73, 135.84, 126.01 (C_q C₆H₄), 128.47, 127.43, 126.13, 112.50 (*o,m*-C₆H₄), 141.73, 127.94 (C₆H₄CH=CH), 124.42 (μ -C=CH), 87.63, 86.90 (C₅H₅), 43.03 (μ -C=CHCH₂), 40.53 (NMe₂) ppm. IR (CH₂Cl₂): ν_{CO} 1991 (vs), 1953 (m), 1786 (s); $\nu_{\text{C}=\text{C}}$ 1524 (m) cm⁻¹. Anal. Calcd for C₃₂H₂₉Fe₂NO₃: C, 65.42; H, 4.94; N, 2.39. Found: C, 65.05; H, 4.99; N, 2.36.

4.5. General Procedure for the Reaction of [(CpFeCO)₂(μ -CO)(μ -C=CHCH₂C₆H₄R)] with [Ph₃C][BF₄] (R = CHO (18**), CH=CHC₆H₄-4-NMe₂ (**19**), CH=CHC₆H₄-4-OMe (**20**)).** An equimolar solution of [Ph₃C][BF₄] in CH₂Cl₂ was added to a cooled solution (-10 °C) of the diiron complex. The reaction mixture was warmed to room temperature and then filtered. The products (**11**, **12**, and **17**) were precipitated from the filtrate by carefully adding Et₂O. Yield: **11**, 63%; **12**, 73%; **17**, 78%.

4.6. HRS Measurements of the First Hyperpolarizabilities. Experimental setup details can be found in ref 20. A Nd:YAG laser with a wavelength of 1064 nm was used as the incident light source. All measurements were carried out in dry CH₂Cl₂ or CH₃CN with sample concentrations of 10⁻⁶–10⁻⁴ M using *p*-NA as the external reference (β (CH₂Cl₂) = 21.6 × 10⁻³⁰ esu,²¹ β (CH₃CN) = 29.2 × 10⁻³⁰ esu²⁵). The compounds were checked for fluorescence using the band-pass filter method described in ref 18.

4.7. X-ray Structure Determination. Suitable crystals for an X-ray structure analysis were obtained from a concentrated THF solution. The data were collected on a Hilger & Watts four-circle diffractometer (Mo K α , λ = 0.710 73 Å). The structures were resolved by direct methods (SHELXL-86).²⁶ Refinement on F^2 was carried out by full-matrix least-squares techniques (SHELXL-93).²⁷ All non-hydrogen atoms were refined with anisotropic thermal parameters. The hydrogen atoms were refined with a fixed isotropic thermal parameter related by a factor of 1.2 to the value of the equivalent isotropic thermal parameter of their carrier atoms. Weights were optimized in the final refinement cycles.

Acknowledgment. This work was supported by the European Community through the TMR Network Contract No. ERBFMRX-CT98-0166 and by the Deutsche Forschungsgemeinschaft.

Supporting Information Available: Tables of X-ray crystallographic data and a packing diagram for compound **17**. This material is available free of charge via the Internet at <http://pubs.acs.org>. Crystallographic data (excluding structure

(25) Kodaira, T.; Watanabe, A.; Ito, O.; Matsuda, M.; Clays, K.; Persoons, A. *J. Chem. Soc., Faraday Trans.* **1997**, *93*, 3039.

(26) Sheldrick, G. M., SHELXL-86: Program for Crystal Structure Determination; University of Göttingen, Göttingen, Germany, 1986.

(27) Sheldrick, G. M., SHELXL-93: Program for Crystal Structure Refinement; University of Göttingen, Göttingen, Germany, 1993.

factors) for the reported structure have also been deposited with the Cambridge Crystallographic Data Centre as supplementary publication no. CCDC-139414. Copies of the data can be obtained free of charge on application to the CCDC, 12

Union Road, Cambridge CB2 1EZ, U.K. (Fax, (internat.) +44-1223-336033; e-mail, deposit@ccdc.cam.ac.uk).

OM000112Z